International Journal of Environment Volume : 04 | Issue : 04 | Oct.-Dec. | 2015
ISSN: 2077-4508 Pages: 278-288

The Study of Various Parameters Affecting the Ion Exchange of Fe(III) Ions from Aqueous Solution on Commercial Cation Ion Exchange Resins

[1]A.A. Swelam, [2]M.A.El-Nawawy, [3]A.M.A.Salem and [4]A.A. Ayman

[1, 2, 3] Department of Chemistry, Faculty of Science, Al-Azhar University, Cairo, Egypt.
[4] Department of basic Science, Faculty of Engineering, Modern University for technology & information, Cairo, Egypt.

ABSTRACT

This work introduces the feasibility of using Amberjet 1500H, Amberjet 1300H and Amberlite IRC86 ion exchange resins as a selective solid phase for the removal of ferric ions from aqueous solution. Amberjet 1500H shows a remarkable increase in sorption capacity for ferric ions compared to other resins used herein. The adsorption process shows maximum removal of ferric in pure aqueous solution for an initial ferric concentration of 5.98 mmol/l. The ferric ions adsorption could be fitted to Langmuir, Freundlich, Temkin and Dubinin–Radushkevich (D-R) isotherms. The adsorption of ferric ions these cation exchange resins follows the pseudo-first-order kinetics, pseudo-second-order kinetics and an Elovich equation. The intraparticle diffusion of copper on ion exchange resins represents the rate-limiting step. The thermodynamics parameters such as $\Delta G°$, $\Delta H°$, and $\Delta S°$ were also evaluated. The uptake of ferric ions by the first two ion exchange resins, have good potential for the removal/recovery of ferric ions from aqueous solutions. We conclude that such ion exchange resins can be used for the efficient removal of ferric ions from water and wastewater.

Key words: Fe(III), Adsorption, Removal, Kinetics, Thermodynamic

Introduction

Water is a vital factor in many industrial processes, including mining, medium for cooling, creating steam, transport or cleaning; it is often an essential component of the process or product. With the right treatment technologies, water can be reused over several cycles which help to bridge the gap between water supply and demand.

The presence of heavy metal ions in water, mostly originating from industrial activities, has a critical impact on the environment and indirectly affects human health and other organisms (Bruce *et al.,* 2015, Gunnar *et al.,* 2015). Heavy metal ions are not biodegradable. Therefore, suitable methods are needed to remove these elements from water. So far, many attempts have been dedicated to the effective removal of heavy metal ions from aqueous solutions and different methods have been developed such as chemical precipitation (Morteza *et al.,* 2015), flotation (Huang *et al.,* 2012) membrane filtration (Jie *et al.,* 2014), liquid extraction (Tien *et al.,* 2013), reverse osmosis (Moti *et al.,* 2015), electrodialysis (Simona *et al.,* 2015), adsorption (Oleksandra et al., 2015), and ion exchange processes (Xiaoyu *et al.,* 2015). Physico-chemical techniques are attractive due to a variety of reasons such as process economics, reliability and ease of use. Iron is one of the most abundant metals of the Earth's crust. It occurs naturally in water in soluble form as ferrous iron (bivalent iron in dissolved form Fe (II) or Fe $(OH)_2^+$) or complexes form like ferric iron (trivalent iron, Fe (III) which precipitates as Fe $(OH)_3$) or even bacterial form. The presence of iron in water can also have an industrial origin, such as metal plating, mining, iron and steel industry, metal corrosion, etc. There are many industrial situations where iron or impurities must be removed from solutions (Ghosh *et al.*, 2008). Iron in drinking water and water supplies cause problems, such as giving reddish colour and odour to water bodies (Cho, 2005**)**. Iron removal is among the most problematic issues for water potabilization, and involves taste, visual effects and clogging, among others. Excess of iron may be present in groundwater or can occur due to corrosion of iron pipes or the residual of iron based coagulants. In raw, fresh water, iron concentration is usually in the range 0–50 mg dm^{-3} (Stegpniak *et al.*, 2008).

In the present study, the elimination of iron (III) ions by Amberjet 1500H, Amberjet 1300H and Amberlite IRC86 cation exchange resins was investigated as a function of different pretreatments, Fe(III) ion concentration, solution acidity, amount of resin, temperature were studied to optimize the conditions for effective removal of ferric ions from aqueous solution. The sorption mechanism was investigated through various adsorption kinetic models including pseudo-first order, pseudo-second order, Elovich and Fickian diffusion models. The activation energy, which is an indicator of the type and mechanism of the sorption

Corresponding Author: A. A. Swelam, Department of Chemistry, Faculty of Science, Al-Azhar University, Cairo, Egypt
E-mail: abdelsamihswelam@yahoo.com

process, was also evaluated using the kinetic constants. Since the evaluation of the heat change of the sorption mechanism is very important for the reactor design, the thermodynamics of the sorption process were also investigated.

Materials and Methods

The following chemicals (Analytical grade) were employed: ferric (III) chloride, hydrochloric acid, sodium hydroxide. Solutions were prepared with redistilled water. All the chemicals were used as purchased, unless otherwise stated.

Resin

A strong-acid cation exchange resin Amberjet 1500H and Amberjet 1300H with the sulphonic acid group ($-SO_3H$) and Amberlite IRC86 with the carboxylic group was used in this work.

Batch experiments

Kinetics experiments were carried out in a thermostated shaker at 20 ± 0.5 ^{0}C and 100 ± 10 rpm. 0.5 g of the resin and 50 ml of ferric chloride aqueous solution were stirred in the shaker. Furthermore the adsorption studies were also carried out by varying time interval (5.0–420 min) at 5.98 mmol/l concentration of the ferric ions to optimize the time required for the removal of this metal ion from its solution. Samples were withdrawn at desired time intervals. Complexometric titration technique was used to determine the Fe(III) concentration in the supernatants after the adsorption onto the resin.

The amount of metal ion adsorbed per unit of adsorbent (q_e) and removal yield (R %) were calculated by Eqs. (1) and (2), respectively:

$$q_e = \frac{(C_o - C_e)V}{W \times 1000} \quad \text{----------} \quad 1$$

$$\text{Removal yield (R \%)} = \frac{C_o - C_e}{C_o} \times 100 \quad \text{----------} \quad 2$$

where q_e is the equilibrium adsorption capacity (mmol g^{-1}), C_o and C_e is the metal ion concentration (mmol L^{-1}) at initial and equilibrium state, respectively, V is the volume of solution (L) and W is the mass (g) of adsorbent.

Results and Discussion

Effect of initial Ferric ion concentration

Fig. 1 exhibits the effect of initial Ferric ions concentration on the % removal efficiency of ferric ions. % Removal efficiency of Fe(III) decreases slightly with increase concentration of initial ferric ions (2.02, 4.06 and 5.98 mmol/l) for Amberjet 1500H may be attributed to that less number of favourable sites for ion exchange are available with the increase of metal ion concentration at a fixed resin dosage. However, the % removal efficiency of ferric ions decreases with the increase of ferric concentration (from 8.08 to 9.98 mmol/L).

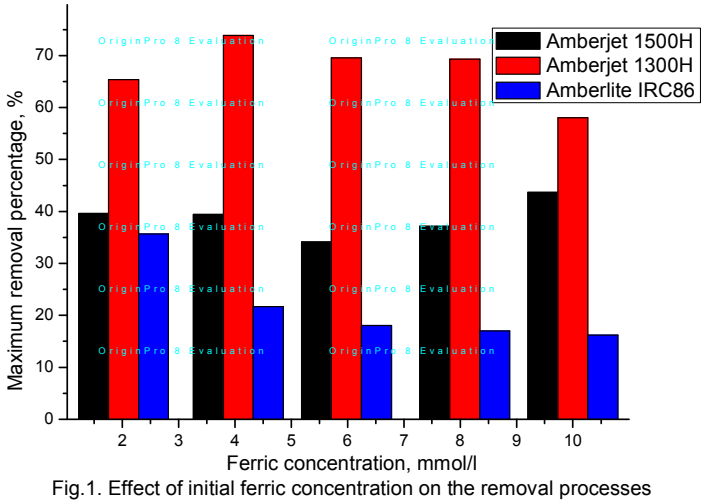

Fig.1. Effect of initial ferric concentration on the removal processes

On the other hand, % removal efficiency of Fe(III) show increases considerably at high initial Fe(III) concentrations for the Amberjet 1300H (2,02 to 4.06 mmol/l) then the % removal efficiency show decreases with increase concentration of initial ferric ions (from 5.98 to 9.98 mmol/L). For aqueous-ferric-Amberlite IRC86, the % removal efficiency show decrease with increase of initial ferric concentration. The slight dependence of % removal on initial Fe(III) concentrations may be ascribed to the high affinity of the present resins to ferric ions, in addition to the higher initial concentration of Fe(III) provides an important driving force to overcome the mass transfer resistance for ferric ions transfer between the solution and the surface of the resins (Ghaedia *et al.,* 2012). The present trend has been found consistent with the reported results by Al-Anber and Al-Anber, 2008; Zewail and Yousef, 2015.

Effect of resin dosage on adsorption

Fig. 2 shows the removal of ferric ions as a function of resin dosage using 1500H, 1300H and IRC86 in an aqueous solution. The resin dosage varied from 0.25 to 8.0 g and equilibrated for 6-7 h. It is clear that, the removal percentage of ferric ions show increase with increase of both Amberjet 1500H and Amberlite IRC86 resins concentration, for the maximum removal percentage of 61.54% of ferric ions by Amberjet 1500H requires a minimum resin dose of 8g and 55.52% for Amberlite IRC86. On the other hand, the removal percentage of ferric ions show increase with increase of Amberjet 1300H resin up to 2.0g, after 2.0g resin, sudden decrease of the uptake percentage with increase of resin dose obtained.

The data clearly show that, the Amberjet 1500H has a high level of performance in terms of the removal of ferric ions. The observed differences in ferric ions uptake by the three resins may be due to the high ion exchange capacity of 1500H, 1300H and low ion exchange capacity of IRC86. The experimental results revealed that the ferric removal efficiency increases up to an optimum dosage beyond which the removal efficiency does change (Rengaraj and Moon, 2002). It may be concluded that by increasing the adsorbent dose the removal efficiency increases but adsorption density decreases. The decrease in adsorption density can be attributed to the fact that some of the adsorption sites remain unsaturated during the adsorption process, whereas the number of available adsorption sites increases by an increase in adsorbent and this results in an increase in removal efficiency. As expected, the equilibrium concentration decreases with increasing adsorbent doses for a given initial ferric concentration, because for a fixed initial solute concentration, increasing the adsorbent doses provides a greater surface area or adsorption sites (Ho *et al.,* 1995).

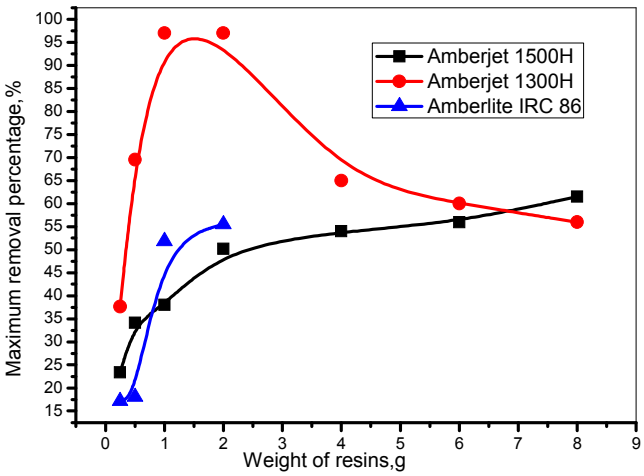

Fig.2. Effect of resin concentration on the removal processes of ferric

The effect of solution acidity on adsorption

The adsorption behaviour of metal ions is significantly influenced by acidity, which affects the ionization of the surface functional groups on resins. In this study, initial acidity for all the experiments were controlled in the range of 0.001-2.0 M HCl to avoid the chemical precipitation of metal ions. Fig. 3 showed the uptake of Fe(III) at different concentration of HCl. An abrupt decrease of adsorption capacity was observed when solution acidity changed from 0.001-1.0 M HCl then no ferric uptake after 0.01M HCl using Amberlite IRC86 as weak cation exchange resin. Whereas, by using both Amberjete 1500H and Amberjete 1300H as strong cation exchange resins, the uptake of ferric has no significant after 1.0 and 2.0 M HCl, respectively.

The adsorption trends could be ascribed to the competition between Fe(III) and hydrogen ions. At low pH, carboxylic groups are present in protonated form and the active sites of the adsorbent are less available for Fe(III) due to greater repulsive forces. Hydrogen ion is the most favourable cation for weak acid resins and excessive hydrogen ions could compete with Fe(III) and further decrease the metal uptake. At intermediate pH values, carboxylic groups on the resin are deprotonated, hence Fe(III) can be adsorbed more effectively by Amberlite IRC86 resin. However, for both Amberjete 1500H and Amberjete 1300H as strong cation exchange resins, Hydrogen ion is the lower favourable cation for sulphonic groups, and excessive hydrogen ions could little compete with Fe(III) than carboxylic groups on the weak resin. Our results agree well with many researches (Ling *et al.,* 2010; Tan *et al.,* 2008; Congcong *et al.,* 2015; Lichun, 2014).

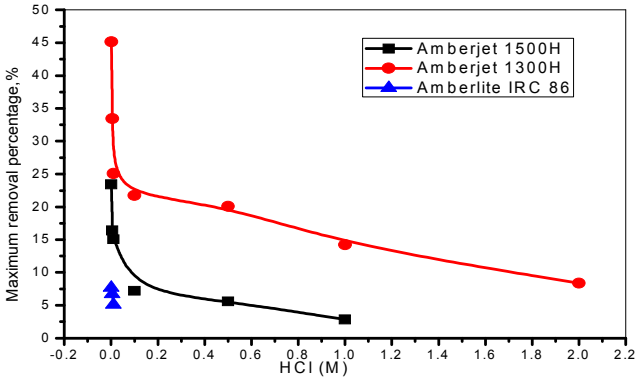

Fig.3. Effect of HCl concentration on the removal processes of ferric

The distribution ratio (D)

Distribution ratio *D* for ferric ions was determined by the batch method at different temperature systems. The distribution ratio, D, is defined as the ratio of metal ion concentration on the resin to that in the aqueous solution and can be used as a valuable tool to study Fe(III) mobility. The distribution ratio *D* is defined by the following relationship:

$$D = \frac{\text{Weight (in mg) of metal ion taken up by 1 g of polymer}}{\text{Weight (in mg) of metal ion present in 1 mL of solution}}$$

Various portions of (500 mg each) the resin were taken in Erlenmeyer flasks and mixed with 50 ml of different metal ion solutions in the aqueous medium and subsequently shaken for 24 h in temperatures controlled shaker at 293, 308 and 318 K to attain the equilibrium.

High values of the distribution ratio as in aqueous-Amberjet 1500H and –Amberjet 1300H systems (with exception of the 318 K - Amberjet 1500H system), D values indicate that the metal has been retained by the solid phase through sorption reactions, while lower values of D (as in aqueous-Amberlite IRC86 system), indicate that a large fraction of the metal remains in solution. Fig. 4 shows that the rapid ferric sorption has significant practical importance, as this will facilitate with the small amount of resins to ensure efficiency and economy (Asif and Shaheen, 2013; Erdem, 2004).

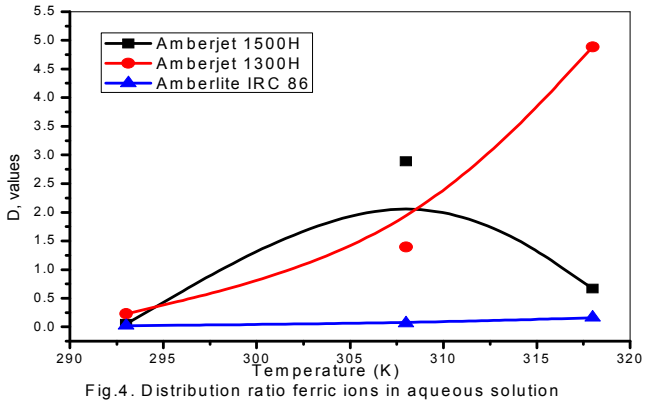

Fig.4. Distribution ratio ferric ions in aqueous solution

Isotherm models of ferric adsorption

The equilibrium adsorption isotherms of ferric ions were determined at three different temperatures (293, 308 and 318 K). The experimental data were fitted to linear equations of Freundlich, Langmuir (Giorgos *et al.,* 2015, Tingshun *et al*., 2015), Dubinin and Radushkevich, 1947 (D-R) and Temkin, 1940 isotherm models.
The Langmuir isotherm is represented by the following equation:

$$\frac{C_e}{q_e} = \frac{1}{K_L Q_{max}} + \frac{C_e}{Q_{max}} \quad \text{----------} \quad 3$$

where C_e (mmol/L) is the equilibrium concentration of metal ions remaining in solution, q_e (mmol/g) is the amount of metal ions adsorbed per weight unit of sorbent after the equilibrium, Q_{max} (mmol/g) is the maximum sorption capacity of metal ions, and K_L (L/mmol) is a constant that relates to the heat of sorption.
The Freundlich model is represented by the following equation:

$$\log q_e = \log K_f + \frac{1}{n} \log C_e \quad \text{----------} \quad 4$$

where k_f represents the sorption capacity when metal ion equilibrium concentration equals 1, and n represents the degree of dependence for sorption with equilibrium concentration.
Another equation used in the analysis of isotherms was proposed by Dubinin and Radushkevich, 1947 **(**D-R**)**.
The D–R equation has the linear expression as follows:

$$\ln q_e = \ln X_{D-R} - \beta\varepsilon^2 \quad \text{----------} \quad 5$$

where q_e is defined as above, X_{D-R} (mmol/g) is the maximum sorption capacity, β is the activity coefficient related to mean sorption energy (mol^2/kJ^2), and ε is the Polanyi potential, which is equal to:

$$\varepsilon = RT \ln\left(1 + \frac{1}{C_e}\right) \quad \text{----------} \quad 6$$

where R is the ideal gas constant (8.3145 J/(mol K)), and T is the absolute temperature (K). The value of E_{D-R} is related to the sorption mean free energy (kJ/mol). The relationship is expressed as:

$$E_{D-R} = \frac{1}{\sqrt{-2\beta}} \quad \text{----------} \quad 7$$

The magnitude of E_{D-R} is useful to estimate the type of sorption reaction. The E_{D-R} value in the range of 1–8 kJ/mol indicates physical adsorption, the value between 8 and 16 kJ/mol signifies an ion-exchange process, its value in the range of 20–40 kJ/mol is indicative of chemisorption (Yongfeng *et al.,* 2015).
The Temkin isotherm equation assumes that the heat of adsorption of all the molecules in layer decreases linearly with coverage due to adsorbent–adsorbate interactions, and that the adsorption is characterized by a uniform distribution of the bonding energies up to some maximum binding energy. The Temkin isotherm has been used in the following form:

$$q_e = \left(\frac{RT}{b_T}\right) \ln A_T + \left(\frac{RT}{b_T}\right) \ln C_e \quad \text{----------} \quad 8$$

Or

$$q_e = B_T \ln A_T + B_T \ln C_e \quad \text{----------} \quad 9$$

where R is gas constant (8.314 J mol^{-1} K^{-1}), T is temperature (K), A_T is the equilibrium binding constant (L g^{-1}) corresponding to the maximum binding energy, and constant $B_T = (RT/b_T)$ is related to the heat of adsorption. A plot of qe versus $\ln C_e$ (Fig. not shown) is used to calculate the Temkin isotherm constants A_T and B_T.
The Langmuir isotherm assumes adsorption at homogeneous sites of the adsorbent with minimal interaction between adsorbed metal ions. The maximum adsorption capacity (Q_{max}) values predicted from the isotherm model for Amberjet 1500H, Amberjet 1300H and Amberlite IRC86 cation exchange resins are shown in Table 1. The total ferric ions intake capacity was best fitted at 293 K for Amberjet 1500H, Amberjet 1300H and Amberlite IRC86 cation exchange resins. The dimensionless separation factor, R_L was obtained as follows;

$$R_L = \frac{1}{(1+K_L C_0)} \quad \text{----------} \quad 10$$

Where, the k_L is Langmuir constant and C_0 is the concentration of initial metal ion. The value of R_L indicates the adsorption nature to be either unfavourable if $R_L > 1$, linear if $R_L = 1$, favourable if $< 0 < R_L < 1$ and irreversible if $R_L = 0$. In addition to regression coefficient R^2 (0.9982 and 0.9912) based on the data fit at both Amberjet 1500H and Amberjet 1300H resins, ferric ion adsorption, follow a Langmuir type monolayer adsorption.
Freundlich isotherm was above unity for the ferric ion uptake (Table 1) which also indicates favourable adsorption by this isotherm onto the resins. It predicted the constant (K_f) for ferric ions uptake by Amberjet 1500H, Amberjet 1300H and Amberlite IRC86, to be 0.3722, 0.4632 and 1.4347 for the three resins used above, respectively. The values of regression coefficient (R^2) also indicated good fitting to this model for Amberlite

IRC86 (R^2 = 0.9996). Based on the data fit at Amberlite IRC86 resin, ferric ion adsorption follows a Freundlich type multilayer adsorption process.
The Temkin model was also fitted well as observed from correlation coefficient R^2 values. The Temkin constant, B_T, related to the heat of adsorption was 0.1277**,** 0.0638 and 0.3378 (J/mol). The value of A_T was obtained maximum as 0.03930, 0.0007 and 0.1440 (L/g) for ferric ions onto the Amberjet 1500H, Amberjet 1300H and Amberlite IRC86, respectively.

Table 1: Adsorption isotherm parameters of Fe (III) on different ion exchange resins in aqueous solution.

Isotherm parameters		Resins		
		Amberjet 1500H	Amberjet 1300H	Amberlite IRC86
Langmuir parameters	Q_{max} (mmol/g)	0.1901	0.4011	0.0673
	K_L (L/mmol)	3.3399	13.9253	0.4758
	R_L	0.0527	0.0122	0.5419
	R^2	0.9982	0.9912	0.9989
Freundlich parameters	n	2.8045	7.7592	0.6438
	K_F	0.3722	0.4632	1.4347
	R^2	0.9520	0.7769	0.9996
Temkin parameters	A_T (L/g)	0.0393	0.0007	0.1440
	B_T (J/mol)	0.1277	0.0638	0.3378
	R^2	0.7913	0.8215	0.9776
D-R parameters	β ($mol^2\ kJ^{-2}$)	3.84×10^{-8}	8.46×10^{-9}	6.86×10^{-7}
	X_{D-R} (mmol/g)	0.2822	0.4513	0.0980
	E (kJ/mol)	3.608	7.687	0.854
	R^2	0.0718	0.2689	0.6598

The mean free energy of sorption (E_{D-R}) calculated by Equation (7) based on the results of Table 1 was found to be 3.608, 7.687 and 0.854 kJ/Mol for ferric ions for Amberjet 1500H, Amberjet 1300H and Amberlite IRC86 respectively. These values are similar to the typical range of bonding energy for physisorption mechanisms (< 8 kJ/mol) (Priyabrata and Banat, 2014). The values indicate that, physical adsorption plays a major role to the intake of ferric ions.

Adsorption kinetics

Kinetic studies were carried out using different models, namely, pseudo-first order, pseudo-second order, Elovich and Fickian diffusion intraparticle models to analyse the experimental data (Giorgos *et al.,* 2015; Shek *et al.,* 2009; Chien and Clayton, 1980; Özacar and Singl, 2005).
The uptake-time curves (Fig. not shown) showed that the maximum uptake followed the order of Amberjet 1500H > Amberjet 1300H > Amberlite IRC86 at all-time intervals under the initial concentration of 5.98 mmol/l. The kinetic curves revealed that the adsorption on the three resins was initially rapid within the first 30 min, reached equilibrium after approximately 240 min and remained constant until the end of the experiment. The adsorption of Amberlite IRC86 was slower than that of Amberjet 1500H and Amberjet 1300H, demonstrated the slowest kinetic profile and the lowest adsorption capacity of ferric, reaching equilibrium after approximately 240 min. The rapid initial uptake indicates that the adsorption process is favourable, whereas the slower rate of uptake to reach equilibrium is due to the diminished availability of free adsorption sites and uptake in the narrow, hindered pore regions.
To further analyse the adsorption kinetics, four models were applied to describe the adsorption kinetics. Each model is expressed as follows;
The pseudo-first-order kinetic model is given as:

$$\log(q_e - q_t) = \log q_{e,1} - k_1 t \quad \text{----------} \quad 11$$

The pseudo-second-order equation is expressed as:

$$\frac{t}{q_t} = \frac{1}{k_2 q_{e,2}^2} + \frac{t}{q_{e,2}} \quad \text{----------} \quad 12$$

$$h = k_2 q_{e,2}^2 \quad \text{----------} \quad 13$$

The Elovich equation
The adsorption data may also be analysed using the Elovich equation (Özacar and Sengil, 2005), which expressed as follows:

$$\frac{dq_t}{dt} = \alpha \exp(-\beta q_t) \quad \text{----------} \quad 14$$

To simplify the Elovich equation, Chien and Clayton (1980) assumed $\alpha\beta \gg 1$ and by applying the boundary conditions $q_t = 0$ at $t = 0$ and $q_t = q_t$ at $t = t$. Eq. (14) becomes:

$$q_t = \frac{1}{\beta}\ln(\alpha\beta) + \frac{1}{\beta}\ln t \quad \text{----------} \quad 15$$

where α is the initial sorption rate constant (mmol/g min), and the parameter β is related to the extent of surface coverage and activation energy for chemisorption (g/mmol) (Shek *et al*., 2009; Wu *et al.,* 2009).

The Fickian diffusion law is expressed as;

$$q_t = k_{id}\, t^{0.5} + C \quad \text{---------- 16}$$

where q_t (mmol/g) is the adsorption capacity at time t, q_e (mmol/g) is the adsorption capacity at equilibrium and h (mmol/(g min)) is the initial adsorption rate constant of pseudo-second-order. k_1 (min^{-1}) and k_2 (g/mmol min) are the adsorption rate constants of pseudo-first-order, and pseudo-second-order isotherms, respectively (Table 2a). Constant k_{id} (mmol/(g $min^{0.5}$) is the intra-particle diffusion rate, and C is the intercept of the plots (Fig. not shown). The kinetic parameters for the adsorption of Fe(III) on different adsorbents are given in Table 2b. Different results were obtained from the kinetic models for the three resins, indicating the different adsorption kinetics for three resins. The pseudo-first-order equation was determined to be the best model for Fe(III) adsorption onto both Amberjet 1500H and Amberjet 1300H, with the highest correlation coefficients ($R^2 > 0.98$) among the four equations (Fig. not shown). From the results also we can observe the pseudo-second-order equation for Amberlite IRC86 was determined to be the best model for Fe(III) adsorption, with the highest correlation coefficients ($R^2 > 0.98$) among the four equations. Therefore, it was indicated that the adsorption rate of Fe(III) depended on the Fe(III) temperatures at the external surface of the adsorbent. When the temperature was increased, the initial adsorption rate h (mmol/(g min)) of Amberjet 1500H, Amberjet 1300H and Amberlite IRC86 also increased from 0.0029 to 0.0199 mmol/(g min), 0.0096 to 0.0162 mmol/(g min) and 0.0167 to 0.0111 mmol/(g min), respectively. The value h for Amberjet 1500H was higher than that of the two resins, suggesting that Amberjet 1500H possesses the fastest kinetics among three investigated resins.

Table 2a: Kinetic parameters of Fe (III) on different ion exchange resins in aqueous solution.

Resins	Temp. K	Pseudo first-order model			Pseudo second-order model			
		$q_{e,1,cal}$ (mmol/g)	K_1 (min^{-1})	R^2	$q_{e,2,cal}$ (mmol/g)	K_2 (g/mmol min)	R^2	H (mmol/g min)
Amberjet 1500H	293	0.1952	0.0097	0.9949	0.2645	0.0413	0.9042	0.0029
	308	0.3794	0.0086	0.9923	0.6066	0.0540	0.9965	0.0199
	318	0.4360	0.0095	0.9765	0.5652	0.0387	0.9926	0.0124
Amberjet 1300H	293	0.3572	0.0110	0.9988	0.4782	0.0422	0.9706	0.0096
	308	0.5939	0.0139	0.9954	0.6335	0.0303	0.9857	0.0122
	318	0.5031	0.0120	0.9717	0.6430	0.0393	0.9935	0.0162
Amberlite IRC86	293	0.0357	0.0157	0.9822	0.1099	1.3835	0.9989	0.0167
	308	0.1831	0.0168	0.9787	0.2499	0.1784	0.9972	0.0111
	318	0.4563	0.0262	0.9476	0.4284	0.0576	0.9868	0.0106

A linear relationship was obtained between q_t, and (ln t) over the whole temperatures of ferric solution (figures are not shown). The correlation coefficients between (0.8736 - 0.9949), (0.9400 - 0.9729) and (0.9957 - 0.9367) for Amberjet 1500H, Amberjet 1300H and Amberlite IRC86, respectively (Table 2b). Additionally, Table 2b lists the kinetic constants obtained from the Elovich equation. The relatively high values of the correlation coefficients in all the points suggest that, the sorption of copper onto the three resins is may be appropriately represented by an Elovich kinetic model.

For Fickian diffusion law, all the correlation coefficients were relatively low and the intercept of plots revealed obvious boundary layer effect (Table 2b). Larger intercept means a greater contribution of surface adsorption as the rate-controlling step. In addition, it was essential for the plots of q_t versus $t^{0.5}$ to go through the origin if the intra-particle diffusion was the sole rate-limiting step. However, all the linear portions did not pass through the origin (all intercepts were in the range of 0.9914-0.9233), indicating that intra-particle diffusion maybe not only the rate-controlling factor (Tan *et al.,* 2003).

Table 2b: Kinetic parameters of Fe(III) on different ion exchange resins in aqueous solution.

Resins	Temp.K	Intraparticle diffusion model			Elovich model		
		K_{id} mmol/(g $min^{0.5}$)	C (mmol/g)	R^2	α	β	R^2
Amberjet 1500H	293	0.0138	-0.0134	0.9914	0.0088	21.4961	0.8736
	308	0.0225	0.1613	0.9330	0.0741	9.9079	0.9949
	318	0.0230	0.0900	0.9661	0.0389	9.9384	0.9750
Amberjet 1300H	293	0.0260	0.0214	0.9973	0.0267	11.1470	0.9408
	308	0.0285	0.0640	0.9737	0.0367	8.6670	0.9400
	318	0.0281	0.1024	0.9610	0.0486	8.5925	0.9729
Amberlite IRC86	293	0.0026	0.0709	0.9415	3.5113	105.4852	0.9957
	308	0.0107	0.0689	0.9292	0.0395	23.7023	0.9882
	318	0.0218	0.0436	0.9233	0.0272	11.8878	0.9357

Amberjet 1500H exhibited the fastest kinetic property for Fe(III) removal among the three studied resins. Compared with Amberjet 1300H, the kinetic superiority of Amberjet 1500H was ascribed to its higher exchange capacity and smaller particle size. On the other hand, Amberjet 1500H and Amberjet 1300H had the same

matrix structure, functional groups and exchange capacity. Compared with the Amberlite IRC86 also which had different matrix structure, functional groups and exchange capacity. This was further evidence indicating that the active sites of the three resins are mainly distributed on the external surface. The adsorption rate of Amberjet 1500H was faster than Amberjet 1300H because of its higher external surface area. Therefore, the external surface of resins was the key factor in the rate-controlling (Yu *et al.,* 2012).

Effect of temperature on thermodynamic parameters

The equilibrium removal of Fe(III) ions as a function of temperature, for experiments conducted at constant concentrations of Fe(III) equal to 5.98 mmol/L. The adsorption of Fe(III) onto the surface of Amberjet1500H, Amberjet1300H and Amberlite IRC86 place quickly regarding the temperature (293–318 K). On the other hand, enhancement of the adsorption capacity of the resins at higher temperatures may be attributed to the activation of the adsorbing surface and increase in the mobility of metal ions. Also, this fact demonstrated an endothermic biosorption process (Blazquez *et al.,* 2005).

The removal percentage of ferric onto the Amberjet 1500H, Amberjet 1300H and Amberlite IRC86 ion-exchange resins (Fig. not shown) was raised from 34.11 to 96.66 %, 69.57 to 77.99% and 18.06 to 61.87% for the three resins, respectively, with increase in temperature from 293 to 318 K. This may be due to the formation of new active sites in the ion-exchange resins to increase in temperature, activation of the adsorbing surface and increase in the mobility of metal ions. The adsorption amount also augmented with an increase of temperature. In aqueous-ferric-Amberjet 1500 system at 318 K, the uptake show decrease and the removal percentage decreased to 86.96%. For the three resins, the amount of Fe(III) adsorbed order generally follows the sequence; Amberjet 1500H > Amberjet 1300H > Amberlite IRC86 at all temperatures under the initial concentration of 5.98 mmol/l, 50 ml ferric solution and 0.5g of each resin. An increase of adsorption capacities of Fe(III) on three resins as the temperature increased (Fig. 5), indicating also an endothermic process and a possible type of chemical adsorption mechanism occurs.

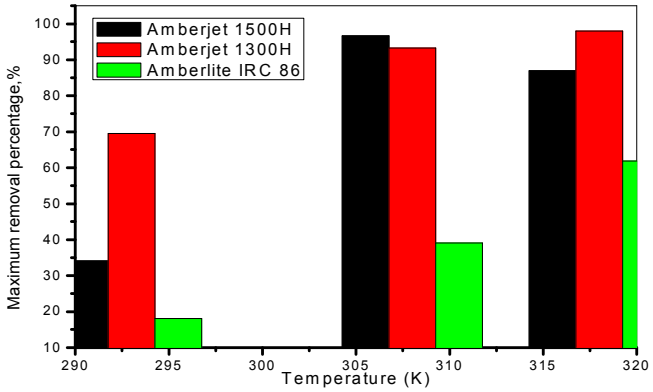

Fig.5. Effect of temperature on the removal processes of ferric

The activation energy provides information about the dependence of the adsorption process with temperature: the greater the activation energy value, the more temperature affects the adsorption process.

To evaluate the nature of the interaction between Fe(III) ions and the Amberjet 1500H and Amberjet 1300H active sites, the value of activation energy obtained (59.764 and 83.434 kJ/mol, Table 3) allows to know the nature of the adsorption process. In this sense, the E_a values fall within the 59.764-83.434 kJ mol^{-1} range generally considered for processes in which chemisorption predominates. This is revealed not only by the high activation energy value but also by the speed of the process (Gladstone *et al., 1941*). Whereas the value of activation energy obtained by Amberlite IRC86 (22.85 kJ/mol, Table 3) allows to know the nature of the adsorption process. In this sense, the E_a values fall within the 5–40 kJ mol^{-1} range, generally, considered for processes in which physisorption predominates. This is revealed not only by the low activation energy value but also by the speed of the process (Gladstone *et al.,* 1941; Blazquez *et al.,* 2005).

In order to further support the assertion that physical adsorption is the predominant mechanism, the values of the activation energy (E_a) and sticking probability (S^*) were estimated from the experimental data. They were calculated using a modified Arrhenius type equation related to surface coverage as expressed in equations:

$$\theta = 1 - \frac{C_e}{C_0} \quad \text{---------- 17}$$

$$S^* = (1-\theta)\exp\left(-\frac{E_a}{RT}\right) \quad \text{---------- 18}$$

The sticking probability, S^*, is a function of the adsorbate/adsorbent system under consideration and is dependent on the temperature of the system. The parameter S^* indicates the measure of the potential of an adsorbate to remain on the adsorbent indefinitely. It can be expressed as in Table 3.

The effect of temperature on the sticking probability was evaluated throughout the temperature range from 293 to 318K by calculating the surface coverage at the various temperatures. Table 3 also indicated that the values of S*≤ 1 for both 1500H and 1300H, hence the sticking probability of the Fe(III) ion onto the two resin systems are very high, while for the IRC86 system, S* was ≥1, hence the manganese ions unsticking to IRC86 surface – no sorption

The apparent activation energy (E_a) and the sticking probability (S^*) are estimated from the plot (Fig. not shown). The positive values of the apparent activation energy E_a also indicated that the higher solution temperature favours the adsorption process and also the adsorption process is endothermic in nature (Singha and Das, 2013).

The study of the temperature effect on Fe(III) removal by the resins enabled us to determine the thermodynamic parameters (ΔG°, ΔH° and ΔS°) of these reactions. The standard Gibbs free energy change, ΔG°, when the adsorption reaches an equilibrium state can be written as follows:

$$\Delta G^{\circ} = -RT\ln(K_d) \quad \text{----------} \quad 19$$

where T is the temperature (K), R is the gas constant (8.314 J mol^{-1} K^{-1}) and K_d denotes the equilibrium constant. Therefore, ΔG° for an adsorption reaction can be estimated if distribution coefficients, K_d, for the adsorption processes are known. Hence, in order to determine the adsorption isotherms at different temperatures (from 293 to 318 K), the concentration initial ferric ions for each temperature was constant value (5.98 mmol/L).

Table 3: Thermodynamic parameters of Fe(III) on different ion exchange resins in aqueous solution.

Thermodynamic parameters	Resins		
	Amberjet 1500H	Amberjet 1300H	Amberlite IRC86
ΔS^0 (J/mol. K)	290	309	176
ΔH^0 (KJ/mol.)	90.995	94.445	61.055
R^2	0.061	0.998	0.982
	ΔG°		
Temp., K	Amberjet 1500H	Amberjet 1300H	Amberlite IRC86
293	7.212	3.595	9.293
308	2.717	0.852	7.027
318	1.071	4.192	4.807
S*	8.92 x 10^{-12}	4.24 x 10^{-16}	7.23 x 10^{-5}
Ea (KJ/mol.)	59.764	83.433	22.850
R^2	0.149	0.990	0.863

The values of the standard Gibbs free energy change, ΔG°, were calculated for each temperature (Table 3). The negative value of ΔG^0 confirms the feasibility of the process and the spontaneous nature of the sorption. It is of note that ΔG° values up to −20 KJ mol^{-1} are consistent with the electrostatic interaction between sorption sites and the metal ion (physical adsorption), while ΔG° values more negative than −40 KJ mol^{-1} involve charge sharing or transfer from the biomass surface to the metal ion to form a coordinate bond (Horsfall *et al.,* 2006). If ΔG° is a positive value at all temperatures accompanied by the positive $\Delta S°$, it can be suggested that the sorption reactions are nonspontaneous with a low affinity and presence of energy barrier also for Fe(III) using Amberlite IRC86. Also, the change in apparent enthalpy, ΔH^0, and entropy ΔS^0 of the adsorption mechanism can be calculated using the following equation:

$$\ln K_d = \frac{\Delta S}{R} - \frac{\Delta H}{RT} \quad \text{----------} \quad 20$$

The Vant'Hoff plot of ln K_d as a function of $(1/T)$ (Fig. not shown) gave a straight line. The calculated slope and intercept from the plot were used to determine ΔH^0 and ΔS^0, respectively (Table 3). In operating times, the values of ΔH^0 are positive, indicating that the sorption reaction is endothermic. The positive values of ΔS^0 show the increasing randomness at the solid/liquid interface during the adsorption process and the entropy is a driving force (Gassan *et al.,* 2013). Al-Anber and Al-Anber, 2008, obtained values for ΔG^0, ΔH^0 and ΔS^0 in the same order for Fe(III) adsorption in a batch system for a temperature range between 293 and 318 K.

Conclusion

The results obtained in this study allow us to state the following:

I. Commercial synthetic cation exchange resin, abundant, and cheap.
II. Commercial synthetic cation exchange resin has considerable potential for the removal of metal ions from effluents not only from pure aqueous solution, but also from other contaminated wastewaters over a wide range of concentrations.
III. The adsorption rate of Fe(III) ions by commercial synthetic cation exchange resin was relatively rapid, stable and occurred in less than 300 min.
IV. Kinetic pseudo-first and pseudo-second order models allow accurate fit of the experimental data.

V. The use of commercial synthetic cation exchange resin straightly without pretreatment for metals adsorption is feasible, and can also be used as metallic cations (iron) adsorbent in industrial applications.
VI. The removal efficiency of Fe (III) ions increases with incrementing temperature.
VII. The activation energy value falls within the range considered for processes when the chemisorption or physisorption predominates, which also accounts for the speed at which the operation occurs.
VIII. The values of thermodynamic functions show that the adsorption of Fe(III) ions onto Commercial synthetic cation exchange resin is spontaneous or nonspontaneous and of endothermic nature.
IX. The adsorption mechanism is predominantly physisorption with some chemisorption also occurring.
X. The adsorption process is environmentally friendly and is able to reduce the iron load from different effluents, and it may further provide an affordable technology for small and medium-scale industry.

References

Al-Anber, Z.A., M.A.S. Al-Anber, 2008. J. Mex. Chem. Soc., 52 (2), pp. 108–115.
Asif, A. K., S. Shaheen, 2013. Solid State Sciences, 16,pp. 158-167.
Blazquez, G., F. Hernainz, M. Calero, L.F. Ruiz-Nuñez, 2005. Process Biochem., 40, pp. 2649–2654.
Bruce, A. F., C. M. Prusiewicz, M. Nordberg, 2015. Metal Toxicology in Developing Countries, Chapter 25; DOI: 10.1016/B978-0-444-59453-2.00025-1, pp. 529–545.
Chien, S.H. and W.R. Clayton, 1980. Soil Sci. Soc. Am. J., 44, pp. 265–268.
Cho, B.Y., 2005. Process Biochem., 40, pp. 3314–3320.
Congcong, S., C. Chen, T. Wen, Z. Zhao, X. Wang, A. Xu, 2015. J.Colloid and Interf. Sci., 456, pp.7-14.
Dubinin, M.M., L.V. Radushkevich, 1947.Chem. Zentr.,1, pp. 875–889.
Erdem, E., N. Karabiner, R. Denat, 2004. J. Colloid Interf. Sci., 280, pp. 309–314.
Fiol, N., I. Villaescusa, M. Martinez, N. Miralles, J. Poch, 2006. J. Serarols; Sep. Purif. Technol., 50, pp. 132–140.
Gassan, H., J.M. Ochando-Pulido, S. B. D. Alami, S. Rodriguez-Vives, A. Martinez-Ferez, 2013. Industrial Crops and Products 49, pp. 526–534.
Ghaedia, M., B. Sadeghiana, A. Amiri Pebdania, R. Sahraeib, A. Daneshfarb, C. Duranc, 2012. Chem. Eng. J. 187, pp. 133-141.
Ghosh, D., H. Solanki, M.K. Purkait, 2008. J. Hazard. Mater., 155, pp. 135–143.
Giorgos, M., D. Mitrogiannis, A. Celekli, H. Bozkurt, D. Georgakakis, C.V. Chrysikopoulos, 2015. Chemical Engineering Journal 259, pp. 806–813.
Glasston, S., K.J. Laidler, H. Eyring, 1941. The Theory of Rate Processes; McGraw-Hill, New York.
Gunnar, F. N., B. A. Fowler, M. Nordberg, 2015. Toxicology of Metals: Overview, Definitions, Concepts, and Trends, Chapter 1; DOI: 10.1016/B978-0-444-59453-2.00001-9, pp. 1–12.
Ho, Y.S., D.A. John Wase, C.F. Forster, 1995. Water Res. 29, 1327-1332.
Ho, Y.S., G. McKay, 1999. Process Biochem., 34 (5), pp. 451–465.
Horsfall, J.M., A.A. Abia, A.I. Spiff, 2006. Bioresour. Technol., 97, pp. 283–291.
Huang, C. , H. Lin, H. Huo, Y. Dong, Q.Xue, L. Cao, 2012. Bioresource Technology 114 , 255–261.
Jie, G., S. Sun, W. Zhu, T. Chung, 2014. Water research 63, 252-261.
Lichun, F., C. Shuang, F. Liu, A. Li, Y. Li, Y. Zhou, H. Song, 2014. J.Hazard. Mater. 272, pp. 102-111.
Ling, P.P., F.Q. Liu, L.J. Li, X.S. Jing, B.R. Yin, K.B. Chen, A.M. Li, 2010. Talanta, 81, 424–432.
Morteza, D., A.hmadpour,T. R.Bastami, 2015. J. Magnetism and Magnetic Materials 375, 177-183.
Moti, K., R. Semiat, G. D Carlos, 2015. Desalination 364, pp. 53–61.
Ngah, W.S., M.A.K.M. Hanafiah, 2008 J. Environ. Sci., 20, pp. 1168–1176.
Nieto, L.M., S.B. Driss, G. Hodaifa, C. Faur, S.R. Vives, J.A. Gimenez, J. Ochando, 2010. Ind. Crop. Prod., 32, pp. 467–471.
Oleksandra, S., L. Belyakova, 2015. J. Hazard. Mater. 283, pp. 643–656.
Özacar, M. and I.A. Sengil, 2005. Process Biochem., 40 , 565–572.
Priyabrata, P., F. Banat, 2014. J. Natural Gas Scie. Eng., 18 , 227-236.
Rengaraj, S.and S. H. Moon, 2002. Water Res. 36, pp. 1783-1793.
Selatnia, A., M.Z. Bakhti, A. Madani, L. Kertous, Y. Mansouri, 2004. Hydrometallurgy, 75, pp. 11–24.
Shek, T.H., A. Ma, V.K.C. Lee, G. McKay, 2009. Chem. Eng. J., 146, pp. 63–70.
Simona, C., A. Radu, V. Purcar, R. Ianchis, A.Sarbu, M. Ghiurea, C. Nicolae, C.Modrogan, D. Vaireanu, A. Périchaud, D. Ebrasu, 2015. Applied Surf. Sci., 329 , 65–75.
Singha, B., S. K. Das, 2013. Colloids and Surf. B: Biointer, 107, pp. 97– 106.
Stegpniak, L., U. Kegpa, E. Stańczyk-Mazanek, 2008. Desalination, 223, pp. 180–186.
Tan, X.L., C.L. Chen, S.M. Yu, X.K. Wang, 2008. Appl. Geochem., 23, 2767–2777.
Tan, Y.S. Ho, G. McKay, 2003. Process Biochem., 38 , pp. 1047–1061.
Temkin, I.M., V. Pyzhev, 1940. Acta Physiochem. SSR 12, pp. 217–222.

Tien, Y., M. Wu, R. Liu, Y. Li, D. Wang, J. Tan, R. Wu, Y. Huang, 2013. Carbohydr. Polym., 83, pp. 743–748.
Jiang, T., W. Liu, Y. Mao, L. Zhang, J. Cheng, M. Gong, H. Zhao, L. Dai, S. Zhang, Q. Zhao, 2015. Chemical Engineering Journal, 259, pp. 603-610.
Wu, F.C., R.L. Tseng, R. Juang, 2009. Chem. Eng. J., 150, pp. 366–373.
Xiaoyu, W., Yi Liu, Yongfeng Liu, Duolong Di, 2015. Colloids and Surf. A: Physicochemical and Engineering Aspects 469 , pp. 141–149.
Yongfeng, Z., Z. Yian, W. Aiqin, 2015. Internat. J. Biological Macromolecules 72, pp. 410–420.
Yu K., C. Gu, S.A. Boyd, C. Liu, C. Sun, B.J. Teppen, H. Li, 2012. Environ. Sci. Technol., 46, pp. 8969–8975.
Zewail, T.M. and N.S. Yousef , 2015. Alexandria Eng. J., 54, pp. 83-90.